Resonance in a Spherical-Circular Microstrip Structure with an Airgap

Kin-Lu Wong, *Member, IEEE,* and Hong-Twu Chen

***Abstract*—The resonance problem of the spherical-circular microstrip structure with an airgap between the substrate layer and the ground conducting sphere is studied by using a rigorous Green's function formulation in the spectral domain and Galerkin's moment method calculation. Complex resonant frequencies are obtained in this study, which provide the resonant frequencies and half-power bandwidth of the structure. From the numerical results, it is found that with the increasing of the airgap thickness, the half-power bandwidth of the structure is considerably increased. This improves the low-bandwidth characteristics of microstrip structures. Details of the numerical results are presented and discussed.**

I. Introduction

In the application of land-mobile satellite communications, spherical microstrip antennas are suitable to be used to overcome the scanning problems involved with the planar patch antennas at low elevation [1], [2]. Several investigations on the spherical-circular microstrip patch antennas have also been reported recently [2]–[4]. In the present paper, we report a possible geometry of the spherical-circular microstrip structure with an airgap between the substrate and ground conducting sphere (see Fig. 1), which improves the low bandwidth characteristics of microstrip structures. Green's function formulation in the spectral domain [3] and Galerkin's moment method [5] are employed in studying the resonant problem of such a geometry. Complex resonant frequencies which provide the resonant frequency and half-power bandwidth of the structure are calculated and analyzed as a function of the airgap thickness. Details of the results for the TM_{11} mode are presented.

II. Theoretical Formulation of the Problem

The geometry of a spherical-circular microstrip structure with an airgap is shown in Fig. 1. The airgap (region 1) is with a thickness of $s\ (=b-a)$ and the substrate (region 2) thickness is $h\ (=c-b)$. The substrate layer is with a relative permittivity. ε_2. A circular patch of radius r_d is mounted on the substrate and the radius of the ground conducting sphere is a. The region of $r>c$ is free space (region 3) with permittivity ε_0 and permeability μ_0. By expanding the wave equations in spherical coordinates, the wave can be decomposed into the TM to $\hat{r}$ and TE to $\hat{r}$ component which are, respectively, generated by the electric potential $A_r\hat{r}$ and magnetic potential $F_r\hat{r}$. These potential in region i $(i=1,2,3)$ can be written as (suppressing $e^{j\omega t}$ time dependence)

$$A_{ri}=e^{jm\phi}\sum_{n=m}^{\infty}A_i(n)\left[\hat{J}_n(k_ir)+\alpha_i(n)\hat{Y}_n(k_ir)\right]P_n^m(\cos\theta)\,, \tag{1a}$$

$$F_{ri}=e^{jm\phi}\sum_{n=m}^{\infty}B_i(n)\left[\hat{J}_n(k_ir)+\beta_i(n)\hat{Y}_n(k_ir)\right]P_n^m(\cos\theta)\,, \tag{1b}$$

Manuscript received August 31, 1992; revised December 18, 1992. This work was supported by the National Science Council of the Republic of China under Contract NSC81-0404-E110-544.

The authors are with the Department of Electrical Engineering, National Sun Yat-Sen University, Kaohsiung, Taiwan 804, Republic of China.

IEEE Log Number 9210210.

with

$$k_i=\omega\sqrt{\mu_0\varepsilon_0\varepsilon_i},\qquad \varepsilon_3=1.0,\qquad \alpha_3(n)=\beta_3(n)=-j$$

where $\hat{J}_n(x)$ and $\hat{Y}_n(x)$ are, respectively, the spherical Bessel functions (Schelkunoff type) of the first and second kind with order n; $P_n^m(x)$ is the associated Legendre function of the first kind with order m and degree n. $A_i(n)$, $\alpha_i(n)$, $B_i(n)$, and $\beta_i(n)$ are unknown coefficients of the harmonic order n to be determined by the boundary conditions at $r=a$, b, and c.

In terms of the aforementioned potential functions, the transverse field components in each region can be obtained. By using the vector Legendre transform introduced in [3], the spectral amplitudes of the transverse field components in region i can then be expressed as

$$\tilde{\tilde{E}}_i(n)=\begin{bmatrix}\frac{k_i}{j\omega\varepsilon_i\varepsilon_0 r}A_i(n)\left[\hat{J}_n'(k_ir)+\alpha_i(n)\hat{Y}_n'(k_ir)\right]\\ \frac{1}{r}B_i(n)\left[\hat{J}_n(k_ir)+\beta_i(n)\hat{Y}_n(k_ir)\right]\end{bmatrix}, \tag{2a}$$

$$\tilde{\tilde{H}}_i(n)=\begin{bmatrix}\frac{k_i}{j\omega\varepsilon_i\mu_0 r}B_i(n)\left[\hat{J}_n'(k_ir)+\beta_i(n)\hat{Y}_n'(k_ir)\right]\\ -\frac{1}{r}A_i(n)\left[\hat{J}_n(k_ir)+\alpha_i(n)\hat{Y}_n(k_ir)\right]\end{bmatrix}. \tag{2b}$$

The prime in the aforementioned equation means a derivative with respect to the argument. To simplify the problem, we define a matrix $\bar{\bar{R}}_i(n)$ satisfying the following relation:

$$\tilde{\tilde{H}}_i(n)=\bar{\bar{R}}_i(n)\tilde{\tilde{E}}_i(n)\,. \tag{3}$$

By substituting (2) to (3), the elements of the matrix $\bar{\bar{R}}_i(n)$ can be obtained and written as

$$\bar{\bar{R}}_i(n)=\begin{bmatrix}0 & R_i^{12}(n)\\ R_i^{21}(n) & 0\end{bmatrix} \tag{4}$$

with

$$R_i^{12}(n)=-j\sqrt{\frac{\varepsilon_0\varepsilon_i}{\mu_0}}\,\frac{\hat{J}_n'(k_ir)+\beta_i(n)\hat{Y}_n'(k_ir)}{\hat{J}_n(k_ir)+\beta_i(n)\hat{Y}_n(k_ir)}\,; \tag{5a}$$

$$R_i^{21}(n)=-j\sqrt{\frac{\varepsilon_0\varepsilon_i}{\mu_0}}\,\frac{\hat{J}_n(k_ir)+\alpha_i(n)\hat{Y}_n(k_ir)}{\hat{J}_n'(k_ir)+\alpha_i(n)\hat{Y}_n'(k_ir)}\,. \tag{5b}$$

Next, by imposing the boundary conditions in the spectral domain, i.e.

$$\tilde{\tilde{E}}_1(n)=[0],\qquad \text{at } r=a\,, \tag{6a}$$

$$\tilde{\tilde{E}}_1(n)=\tilde{\tilde{E}}_2(n),\qquad \text{at } r=b\,, \tag{6b}$$

$$\tilde{\tilde{H}}_1(n)=\tilde{\tilde{H}}_2(n),\qquad \text{at } r=b\,, \tag{6c}$$

$$\tilde{\tilde{E}}_2(n)=\tilde{\tilde{E}}_3(n),\qquad \text{at } r=c\,, \tag{6d}$$

$$\tilde{\tilde{J}}_s(n)=\begin{bmatrix}0 & -1\\ 1 & 0\end{bmatrix}\left[\tilde{\tilde{H}}_3(n)-\tilde{\tilde{H}}_2(n)\right],\qquad \text{on the patch} \tag{6e}$$

where $\tilde{\tilde{J}}_s(n)$ is the spectral amplitude of the surface current density on the patch, the relationship of the surface current density and the tangential electric field on the patch can be derived to be

$$\tilde{\tilde{J}}_s(n)=\bar{\bar{Y}}(n)\tilde{\tilde{E}}_s(n),\qquad \bar{\bar{Y}}(n)=\begin{bmatrix}Y_{11}(n) & 0\\ 0 & Y_{22}(n)\end{bmatrix}. \tag{7}$$

The elements in the $\bar{\bar{Y}}$ matrix are expressed as

$$Y_{11}(n)=-R_3^{21}(n)+R_2^{21}(n)\,, \tag{8a}$$

$$Y_{22}(n)=R_3^{12}(n)-R_2^{12}(n) \tag{8b}$$

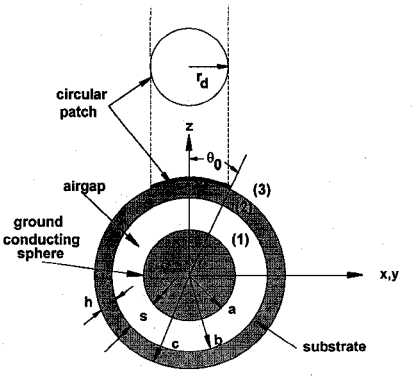

Fig. 1. Geometry of a spherical-circular microstrip structure with an airgap.

with

$$\alpha_1(n) = -\hat{J}_n'(k_1 a)/\hat{Y}_n'(k_1 a),$$

$$\beta_1(n) = -\hat{J}_n(k_1 a)/\hat{Y}_n(k_1 a),$$

$$\alpha_2(n) = -\frac{R_1^{21}(n)\hat{J}_n'(k_2 b) + j\sqrt{\varepsilon_0\varepsilon_2/\mu_0}\,\hat{J}_n(k_2 b)}{R_1^{21}(n)\hat{Y}_n'(k_2 b) + j\sqrt{\varepsilon_0\varepsilon_2/\mu_0}\,\hat{Y}_n(k_2 b)}$$

$$\beta_2(n) = -\frac{R_1^{21}(n)\hat{J}_n(k_2 b) + j\sqrt{\varepsilon_0\varepsilon_2/\mu_0}\,\hat{J}_n'(k_2 b)}{R_1^{21}(n)\hat{Y}_n(k_2 b) + j\sqrt{\varepsilon_0\varepsilon_2/\mu_0}\,\hat{Y}_n'(k_2 b)}$$

The expressions of Y_{11} and Y_{22} can be reduced to the corresponding results in [3], when setting $\varepsilon_1 = \varepsilon_2$, $k_1 = k_2$, i.e., no airgap is present. Then, by following the Galerkin's procedure [5], [6] (expanding the surface current density on the patch with a set of orthogonal functions and weighting (7) with the same set of functions), using the Parseval's theorem [3], and applying the boundary condition that the surface current and the electric field are complementary to each other on the surface of $r = b$, we have

$$[Z][I] = [0]. \tag{9}$$

The elements in $[I]$ are the unknown coefficients of the expansion functions and the elements in $[Z]$ are written as

$$Z_{ij} = \sum_{n=m}^{\infty} \tilde{\tilde{J}}_i^*(n) s(n,m) \bar{\bar{Y}}^{-1} \tilde{\tilde{J}}_j(n) \tag{10}$$

with

$$s(n,m) = \frac{2n(n+1)(n+m)!}{(2n+1)(n-m)!}.$$

The superscript * denotes the complex conjugate transpose and $\tilde{\tilde{J}}_i(n)$ is the spectral amplitude of the ith expansion function. A convenient choice of the expansion functions is the cavity-mode functions derived in [3]. For the existence of nontrivial solutions for $[I]$ in (9), the determinate of $[Z]$ must vanish, i.e.,

$$\det([Z]) = 0. \tag{11}$$

The solutions to (11) are then found to be satisfied by complex frequencies $f = f' + jf''$, which give the resonant frequency f' and the half-power bandwidth $2f''/f'$ for the microstrip structure.

III. Numerical Results and Discussion

In this section, typical numerical results of the complex resonant frequency at TM_{11} mode are presented. The substrate is selected to be with $\varepsilon_2 = 2.32$ and $h = 1.59$ cm. The radius of the circular patch is $r_d = 5$ cm. The effects of introducing an airgap of $\varepsilon_1 = 1.0$ between the substrate and the ground conducting sphere are first discussed in Fig. 2, where the real and imaginary parts of the complex

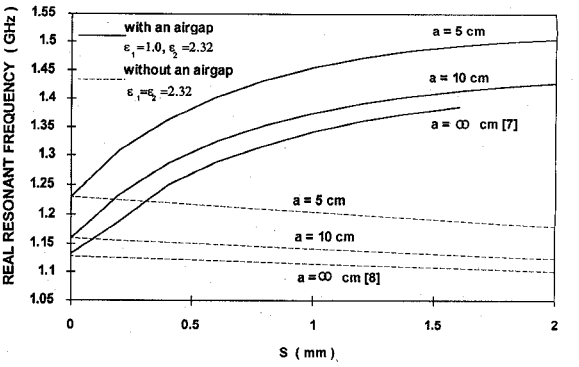

(a)

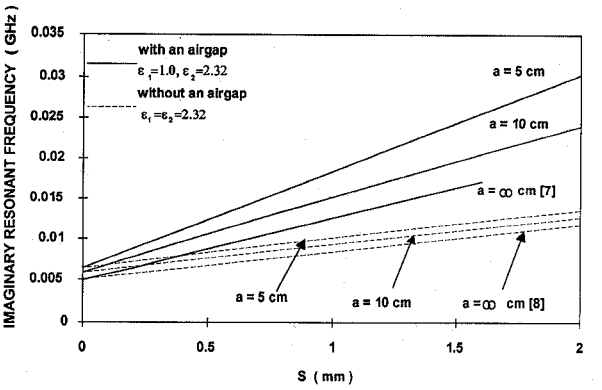

(b)

Fig. 2. (a) Real and (b) Imaginary parts of the complex resonant frequencies for the microstrip structure with $\varepsilon_2 = 2.32$, $h = 1.59$ cm, $r_d = 5$ cm, $\varepsilon_1 = 1.0$ (airgap) or 2.32, $a = 5$, 10 cm and ∞ (planar case).

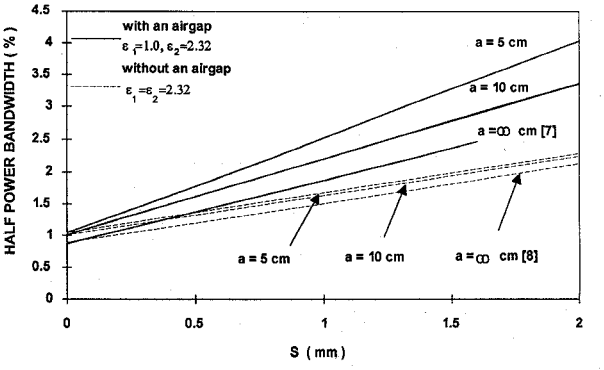

Fig. 3. Half-power bandwidth of the spherical-circular microstrip structure for the case in Fig. 2.

resonant frequencies are shown. The planar case ($a = \infty$ cm) is also presented for comparison. For both spherical and planar structure, two cases of $\varepsilon_1 = 1.0$, $\varepsilon_2 = 2.32$ (region 1 is an airgap) and $\varepsilon_1 = \varepsilon_2 = 2.32$ (region 1 is the same dielectric material as in region 2, i.e., the substrate thickness is now $s + h$) are presented. The results of the planar circular microstrip structure ($a = \infty$ cm) for the cases of with and without an airgap are, respectively, obtained in [7] and [8]. On the other hand, the results of the spherical-circular microstrip structure are obtained in the present paper. The correctness of our numerical calculation has also been verified by obtaining the same results described in [3] for the case of without the airgap. For brevity, these results are not shown here. From the results in Fig. 2(a) for the case of $\varepsilon_1 = 1.0$, $\varepsilon_2 = 2.32$, it is seen that, initially, the

resonant frequency is increased as s increased. This behavior is quite different from that for the case of $\varepsilon_1 = \varepsilon_2 = 2.32$, where the resonant frequency is decreased as s is increased. This is probably due to the effective permittivity of the region under the patch being lowered with the existence of the airgap. As for the imaginary resonant frequencies, the results are shown in Fig. 2(b). It is seen that with an airgap the imaginary resonant frequency is higher, i.e., the radiation loss of the structure is increased. The spherical structure is also seen to be a more efficient radiator than the planar structure. Fig. 3 shows the half-power bandwidth of the microstrip structure for the case in Fig. 2. The bandwidth is seen to be considerably increased due to the existence of an airgap and the spherical structure is also with a higher bandwidth as compared to the planar structure.

IV. Conclusions

The geometry of the spherical-circular microstrip structure with an airgap is studied. Complex resonant frequencies at TM_{11} mode for both the spherical and planar structures are presented. Results indicate that the radiation loss of the microstrip structure increases as the airgap thickness is increased and the spherical structure with an airgap is also a more efficient radiator than the planar structure with an airgap. Furthermore, the half-power bandwidth of the microstrip structure is considerably increased due to the existence of an airgap, and the bandwidth of the spherical structure is also greater than that of the planar structure. This improves the low bandwidth characteristics of the microstrip structure.

References

[1] J. James and P. Hall eds., *Handbook of Microstrip Antennas.* London: Peregrinus 1989, ch. 6.

[2] B. Ke and A. A. Kishk, "Analysis of spherical circular microstrip antennas," *IEE Proc. H,* vol. 138, pp. 542–548, 1991.

[3] W. Y. Tam and K. M. Luk, "Resonance in spherical-circular microstrip structures," *IEEE Trans. Microwave Theory Tech.,* vol. MTT-39, pp. 700–704, 1991.

[4] K. L. Wong, H. T. Chen, and W. L. Huang, "Resonance and radiation of a spherical circular microstrip patch antenna on a uniaxial substrate," *Proc. Natl. Sci. Counc.,* vol. 17, pp. 64–70, 1993, .

[5] R. F. Harrington, *Field Computation by Moment Method.* New York: Macmillan, 1968.

[6] K. L. Wong, Y. T. Cheng, and J. S. Row, "Resonance in a superstrate-loaded cylindrical-rectangular microstrip structure," *IEEE Trans. Microwave Theory Tech.,* vol. MTT-41, May, 1993.

[7] W. Y. Tam and K. M. Luk, "Spectral domain analysis of microstrip antennas with an airgap," *Microwave Optical Tech. Lett.,* vol. 3, pp. 391–393, 1990.

[8] Q. Liu and W. C. Chew. "Curve fitting formulas for fast determination of accurate resonant frequency of circular microstrip patched," *IEE Proc. H,* vol. 135, pp. 289–292, 1988.

Useful Bessel Function Identities and Integrals

E. B. Manring and J. Asmussen, Jr.

***Abstract*—A number of previously unpublished Bessel function identities and indefinite integrals are listed. These are useful in solving electromagnetics problems in cylindrical coordinates, including energy and power calculations, and mode orthogonalization in lossy media. Using these integrals in conjunction with two previously published indefinite Bessel function integrals, two orthogonality integrals are derived. Values of the indefinite integrals at limits of zero and infinity are also given.**

I. Introduction

Often in the solution of electromagnetics problems in cylindrical coordinates, products of Bessel functions are encountered in indefinite integrals or elsewhere. Examples are orthogonalization integrals of modal expansions for matching fields across discontinuities, calculation of power dissipated and energy stored in cylindrical waveguides and cavities, or similar calculations for cylindrical dielectric waveguides [1]. While there are tabulated solutions to certain of these integrals [2], [3], some cannot be found in common references.

The integrals given in [1] are needed in energy and power calculations in geometries of circular symmetry with lossless materials. However, in lossy media, the radial wavenumbers, k_ρ, are complex. In that case $k_\rho \neq k_\rho^*$ and the integrals in [1] cannot be used. Two new indefinite integrals are given below which account for the $k_\rho \neq k_\rho^*$ case. These integrals are also needed when using one mode to orthogonalize a modal series expansion of electric or magnetic fields in a waveguide or cavity at an axial junction. In addition to these integrals, three recurrence identities and another indefinite integral are listed which may be useful in other instances. Since indefinite integrals are often evaluated at limits of zero and infinity, the values of the integrals at these limits are enumerated here. Employing the limiting case at zero for the ordinary Bessel function integral in conjunction with one of the integral identities in [1], certain orthogonality properties of the ordinary Bessel functions may be derived. Two of them, which appear in orthogonality integrals for homogeneously loaded waveguides, are given below.

II. Indefinite Integrals

Given F_ν and G_ν, such that

$$\begin{aligned} F_\nu(\alpha z) &= AJ_\nu(\alpha z) + BY_\nu(\alpha z), \\ F_\nu'(\alpha z) &= AJ_\nu'(\alpha z) + BY_\nu'(\alpha z) \\ G_\nu(\beta z) &= CJ_\nu(\beta z) + DY_\nu(\beta z), \\ G_\nu'(\beta z) &= CJ_\nu'(\beta z) + DY_\nu'(\beta z) \end{aligned} \tag{12}$$

where J_ν and Y_ν are ordinary Bessel functions of the first and second kinds with complex arguments, and ν is an arbitrary complex constant, it is possible to show that

$$\begin{aligned} \int \left[F_\nu'(\alpha z)G_\nu'(\beta z) + \frac{\nu^2}{\alpha\beta z^2} F_\nu(\alpha z)G_\nu(\beta z)\right] z\, dz \\ = \frac{z}{\alpha^2 - \beta^2}\left[\alpha F_\nu(\alpha z)G_\nu'(\beta z) - \beta F_\nu'(\alpha z)G_\nu(\beta z)\right], \\ \alpha \neq \beta. \end{aligned} \tag{13}$$

Since the Hankel functions $H_\nu^{(1)}$ and $H_\nu^{(2)}$ are linear combinations of J_ν and Y_ν, (2) is also true if F_ν and G_ν contain linear combinations

Manuscript received November 13, 1992; revised January 25, 1993.

The authors are with the Department of Electrical Engineering, Michigan State University, East Lansing, MI 48824-1226.

IEEE Log Number 9210212.